

Correlation of spontaneous emission in a one-dimensional random medium with Anderson localization

Peijun Yao, Chuanhong Zhou, Lina Shi, and Xunya Jiang*

State Key Laboratory of Functional Materials for Informatics, Shanghai Institute of Microsystem and Information Technology, Chinese Academy of Sciences, Shanghai 200050, People's Republic of China

(Received 27 January 2007; revised manuscript received 4 April 2007; published 15 May 2007)

Under Anderson localization, two types of correlation of spontaneous emission in one-dimensional random media are investigated: i.e., time-domain field correlation $C_t^E(\mathbf{r}_1, \mathbf{r}_2, \tau)$ and energy-spectrum correlation $C_\omega^P(\mathbf{r}_1, \mathbf{r}_2, \Delta\omega)$. The results show that the spatial correlation length of $C_t^E(\mathbf{r}_1, \mathbf{r}_2, \tau=0)$ is unrelated to the localization length; however, the increase of the correlation length of $\max_\tau |C_t^E(\mathbf{r}_1, \mathbf{r}_2, \tau)|$ with the localization length is sensitive and monotonous. In particular, we find that the fields at the different locations keep on exchanging with each other in a certain fixed speed by investigation of time-domain field correlation. The speed is almost not affected by the random strength and almost equal to the group velocity of the corresponding periodic structure. Therefore the localized mode is really a dynamic equilibrium state though the energy of the localized mode is localized. In addition, because it is not convenient to characterize the localization length by $C_t^E(\mathbf{r}_1, \mathbf{r}_2, \tau)$, another correlation—energy-spectrum correlation $C_\omega^P(\mathbf{r}_1, \mathbf{r}_2, \Delta\omega)$ —is proposed. By investigation of the energy-spectrum correlation for $\Delta\omega=0$, we obtain that there is an approximately linear relation between the spatial correlation length of energy-spectrum and the localization length. Obviously, in the aspect of characterizing the localization length, the energy-spectrum correlation is more convenient than the time-domain field correlation.

DOI: [10.1103/PhysRevB.75.205111](https://doi.org/10.1103/PhysRevB.75.205111)

PACS number(s): 71.55.Jv, 42.25.Dd, 72.15.Rn

I. INTRODUCTION

Light traveling in a disordered medium exhibits some fundamental features which are very different from simple systems and ordered structures,^{1,2} such as diffusion localization, coherent backscattering, and correlations and fluctuations in the speckle pattern. Among them, Anderson localization^{3,4} is still one of the challenging problems, attracting an increasing interest of theoretical and experimental physicists. Ohm's law shows that the transmission of an electron in metal through a slab of length L is proportional to $1/L$. However, when the wavelike nature of the diffusing particles is taken into account, the transmission will be significantly impaired due to the constructive interference of waves in the paths which obey time-reversal invariance. Therefore the diffusion constant will also be reduced significantly and even approach zero when scattering is strong enough.⁵ Anderson predicted the destruction of diffusion and showed that the quantum wave of a particle in a random potential can be localized in space, which turns a conductor into an insulator.⁶ Soon, this phenomenon was generalized to the realm of electromagnetic waves,⁷⁻¹⁰ as well as other classic waves.¹¹⁻¹³ So far, the observation of Anderson localization of classical waves remains a subject of debate, primarily because a suitable system is hard to find and the observation is often obscured by such effects as residual absorption and scattering attenuation. In addition, by using a generalized master equation, Florescu and John¹⁴ have investigated the second-order correlation in light emission of a random laser¹⁵⁻¹⁷ before lasing and after lasing. We are of the opinion that studying other statistical properties will benefit our insight into Anderson localization.

In this paper, we will explore the time-domain field correlation (TDFC) and the energy-spectrum correlation (ESC) of spontaneous emission under Anderson localization and

also investigate the static and dynamic properties of the localized modes by correlations of spontaneous emission. Here, we would like to emphasize that our sources of spontaneous emission are evenly and randomly dispersed inside the system so that all the modes in our system (even deep inside the system) can be excited homogeneously, which is different from the usual research way—one excites the inner modes by the external source and then detects the outer fields to investigate the inner properties of the system. The field induced by the spontaneous emission can better help us to probe into the properties of the inner modes deeper inside the system, especially under Anderson localization. Since our research is focused on simulating the real spontaneous emission inside random active media, it can be directly observed in experiment and valuable in physics. In fact, such a system with homogenous spontaneous emission can easily be realized in experiment as long as the gain of the active system with absorption is much smaller than the lasing threshold. In addition, it is noted that the modes in our system are actually quasilocalized and the field induced by the spontaneous emission will not be divergent because the system is finite.

Usually, conventional correlations¹⁸⁻²⁴ in random media refer to the correlation function of intensity, $C = \langle \delta I(\mathbf{r}, \omega) \delta I(\mathbf{r} + \Delta\mathbf{r}, \omega + \Delta\omega) \rangle / \langle I(\mathbf{r}, \omega) \rangle \langle I(\mathbf{r} + \Delta\mathbf{r}, \omega + \Delta\omega) \rangle$, and that of field $C_E = \langle E^*(\mathbf{r}, \omega) E(\mathbf{r} + \Delta\mathbf{r}, \omega + \Delta\omega) \rangle / \langle I(\mathbf{r}, \omega) \rangle^{1/2} \langle I(\mathbf{r} + \Delta\mathbf{r}, \omega + \Delta\omega) \rangle^{1/2}$. The above formulas are suitable in mesoscopic systems or close to the onset of Anderson localization. However, the objects investigated here are under Anderson localization ($L \gg \xi$), so the cumulant correlations C and C_E become inconvenient. Thus other correlations are attempted, including TDFC and ESC. The TDFC (i.e., coherence²⁵) is

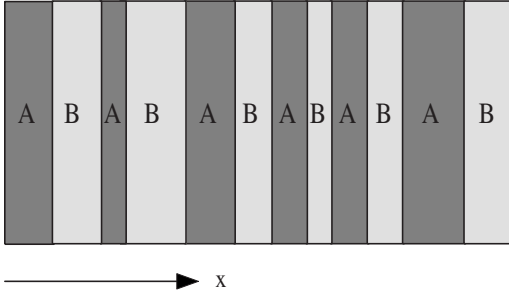


FIG. 1. Geometrical structure of our model. The layers are infinite in extent in the yz plane.

$$C_t^E(\mathbf{r}_1, \mathbf{r}_2, \tau) = \frac{\int E^*(\mathbf{r}_1, t)E(\mathbf{r}_2, t + \tau)dt}{\sqrt{\int |E(\mathbf{r}_1, t)|^2 dt \int |E(\mathbf{r}_2, t)|^2 dt}}. \quad (1)$$

The formula for the ESC, on the other hand, is constructed as follows: for a random field $E(t)$, the amplitude of the component with frequency ω is the Fourier transform $E(\omega) = \int_{-\infty}^{\infty} E(t)\exp(-j2\pi\omega t)dt$. The average energy per unit area of those components with frequencies in the interval between ω and $\omega + d\omega$ is $|E(\omega)|^2 d\omega$, so that $|E(\omega)|^2$ represents the energy spectral density of the light. The ESC is then defined as

$$C_\omega^P(\mathbf{r}_1, \mathbf{r}_2, \Delta\omega) \equiv \frac{\int |E(\mathbf{r}_1, \omega)|^2 |E(\mathbf{r}_2, \omega + \Delta\omega)|^2 d\omega}{\sqrt{\int |E(\mathbf{r}_1, \omega)|^4 d\omega \int |E(\mathbf{r}_2, \omega)|^4 d\omega}}. \quad (2)$$

Generally, researchers are interested in calculating average quantities in random media. So are these authors. We will focus our attention on the quantities $\langle C_\omega^P \rangle$ and $\langle C_t^E \rangle$, where $\langle \dots \rangle$ represents a twofold average: self-average and configurational average; i.e., we will first average them spatially in single configuration, then average them over different configurations. The content of the paper is as follows: In Sec. II, we present the investigated model and the simulation scenario. Section III is devoted to the average TDFC $\langle C_t^E \rangle$. In Sec. IV, we calculate the average ESC $\langle C_\omega^P \rangle$. Our conclusions are summarized in Sec. V.

II. MODEL

As shown in Fig. 1, our one-dimensional random system is made of binary layers with dielectric constants $\varepsilon_a=4.0$ and $\varepsilon_b=1.0$, and the layer thickness is random, $La(Lb)=(1+\gamma \times u) \mu\text{m}$, amid them, u is random strength, and γ is a random number evenly distributed in $[-0.5, 0.5]$. The system totally consists of 1000 pairs of binary layers. Obviously, this structure possesses a periodic background; thus, those localized modes in the band-gap region simultaneously contain the deviation of both band gap and disorder, and the smaller the random strength, the more prominent the effect of period.

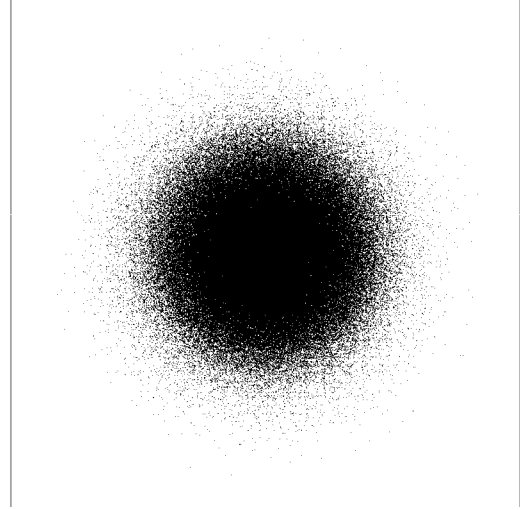


FIG. 2. The statistical distribution of our spontaneous emission source which is a narrow-band Gaussian noise.

In order to exclude the band-gap effect, we set the investigated frequency region (i.e., spontaneous emission frequency range) in the band of rigorously periodic structure. The spontaneous emission current sources are added by the way of the effective electric current J , which are composed of randomly generated sine-wave pulses.²⁶ For concreteness, for a random-generated sine-wave pulse with random starting phase φ_i , starting time t_i , and random pulse length t_{pi} , we can represent it with $\sin[\omega_0(t-t_i) + \varphi_i]$, $t_i < t < t_i + t_{pi}$; then, the effective random current is composed of many such sine-wave pulses: i.e., $J = \sum_i \sin[\omega_0(t-t_i) + \varphi_i]$, which possesses average pulse length t_p . The source generated in this way is a quasimonochromatic field with the central frequency ω_0 . The larger t_p , the narrower its spectral width. In our simulation, the central frequency of spontaneous emission $\omega_0 = 1.885 \times 10^{15} \text{ s}^{-1}$, which lies in the middle of the third band of the rigorous periodic structure. In fact, the complex amplitudes of the sources generated above are correlative in time domain and present a Gaussian distribution in statistics. Figure 2 shows the complex phasor amplitude at one instant of time. By statistics, the probability distribution of the complex phasor amplitude comes to a ‘‘Gaussian molehill,’’ which manifests the source generated in the above way is a narrow-band Gaussian noise source indeed. In our finite-difference time-domain (FDTD) simulation, to get flat spectra, each random source is composed of nine narrow-band Gaussian noise sources with different central frequencies which slightly deviate from ω_0 . Its relative width of spectrum $\Delta\omega_0/\omega_0$ is 1.0%; thus, about dozens of modes will be excited in our system. In addition, the perfect-matched-layer absorbing boundary condition is used in the FDTD algorithm, and spatial interval $\delta x = 0.025 \mu\text{m}$, time step $\delta t = 8.33 \times 10^{-17} \text{ s}$.

III. TIME-DOMAIN FIELD CORRELATION

In this section, the dependence of the average TDFC on the spatial interval for different random strengths u is calculated by a numerical method and explored theoretically. First

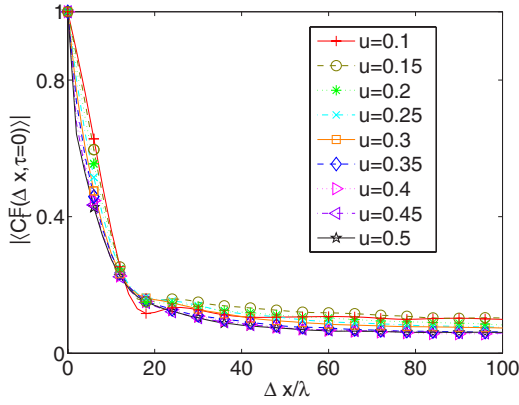


FIG. 3. (Color online) The average TDFC $|\langle C_t^E(\Delta x, \tau=0) \rangle|$ versus the spatial interval Δx for different random strengths u .

of all, we generate a random configuration corresponding to a certain specified random strength u , then add some random spontaneous emission stated above and simulate it with the FDTD algorithm. In the end, we process the simulation results by Eq. (1). For each random strength u , we average 20 configurations at least. After the average, the correlation is a function of $\Delta \mathbf{r}$ ($=\mathbf{r}_2-\mathbf{r}_1$). In the following, we will investigate the average TDFC in two scenarios: spatial TDFC for $\tau=0$ and spatial TDFC for $\tau \neq 0$.

A. Spatial TDFC for $\tau=0$

Figure 3 shows the average TDFC $|\langle C_t^E(\Delta x=x_2-x_1, \tau=0) \rangle|$ versus the spatial interval Δx for different random strengths u . Contrary to our intuition, the correlation shows no relation with the random strength u or the localization length ξ ; nor is sensitive to them. We know that the localized modes will overlap with each other in space and frequency,²⁷ which is also consistent with our numeric results. Figure 4 shows the spectral comparison of two different locations in a single realization; obviously, a similarity between them does exist. In order to uncover the dilemma, we represent C_t^E in frequency form. According to Parseval's theorem, we have

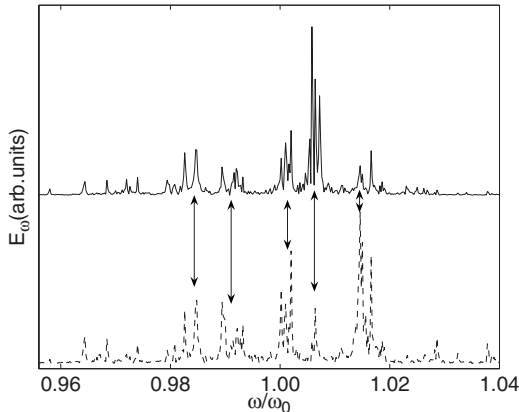


FIG. 4. The spectral comparison between two different locations with the interval $\Delta x=25\lambda$ in a certain realization of random strength $u=0.3$. The double arrows indicate the similarity between them.

$$C_t^E(\mathbf{r}_1, \mathbf{r}_2, \tau=0) = \frac{\int E^*(\mathbf{r}_1, \omega) E(\mathbf{r}_2, \omega) d\omega}{\sqrt{\int |E(\mathbf{r}_1, \omega)|^2 d\omega \int |E(\mathbf{r}_2, \omega)|^2 d\omega}}. \quad (3)$$

Obviously, $C_t^E(\mathbf{r}_1, \mathbf{r}_2, \tau=0)$ is also a spatial frequency-domain field correlation. For arbitrary location in our system, $E(\mathbf{r}, t)$ can be written as

$$E(\mathbf{r}, t) = E(x, t) = \sum_i E(x, \omega_i) e^{-i(\omega_i t + \phi_i)}, \quad (4)$$

where ω_i is the frequency of the i th localized mode, ϕ_i is the phase of the i th localized mode, and $E(x, \omega_i)$ is the complex amplitude; in fact, it is a real number. Here, \mathbf{r} is replaced by x for the investigated object is a one-dimensional system. Hence, $C_t^E(x_1, x_2, \tau=0)$ can be expressed in the following form:

$$C_t^E(x_1, x_2, \tau=0) = \frac{\sum_i E(x_1, \omega_i) E(x_2, \omega_i)}{\sqrt{\sum_i |E(x_1, \omega_i)|^2 \sum_i |E(x_2, \omega_i)|^2}}. \quad (5)$$

In addition, we notice that there is a spatial carrier frequency for $E(x, \omega_i)$: namely,

$$E(x, \omega_i) = f_i(x) \sin(k_i x + \varphi_i), \quad (6)$$

where k_i is the spatial carrier frequency and $f_i(x)$, which possesses approximately exponential form with central peak, is a slowly varied quantity. Then the numerator of the right-hand side of Eq. (5) can be expressed as

$$\sum_i E(x_1, \omega_i) E(x_2, \omega_i) = \frac{1}{4} \sum_i f_i(x_1) f_i(x_2) (e^{ik_i(x_1-x_2)} + e^{-ik_i(x_1-x_2)} - e^{i[k_i(x_1+x_2)+2\varphi_i]} - e^{-i[k_i(x_1+x_2)+2\varphi_i]}). \quad (7)$$

The third and fourth terms on the right-hand side of Eq. (7) will be canceled out because of the random phase φ_i ; then, the first and second terms are left. Thus the net result is

$$C_t^E(x_1, x_2, \tau=0) = \frac{1}{2} \frac{\sum_i f_i(x_1) f_i(x_2) (e^{ik_i(x_1-x_2)} + e^{-ik_i(x_1-x_2)})}{\sqrt{\sum_i |f_i(x_1)|^2 \sum_i |f_i(x_2)|^2}}. \quad (8)$$

So we can know that $C_t^E(x_1, x_2, \tau=0)$ is mainly determined by the spatial interval (x_1-x_2) and k_i , whereas $f_i(x_1) f_i(x_2)$ which is related with the localization length will be mainly reflected in the peak value of $\sum_i E(x_1, \omega_i) E(x_2, \omega_i)$ because it is a slowly varied quantity. Obviously, after normalization, $|C_t^E(x_1, x_2, \tau=0)|$ decreasing with Δx will only depend on the range of k_i which is irrelevant with the localization length; i.e., the correlation length of $C_t^E(x_1, x_2, \tau=0)$ does not depend on the localization length. In general, it is the stochastic property of k_i and the cancellation between the different localized mode smashing the correlations although

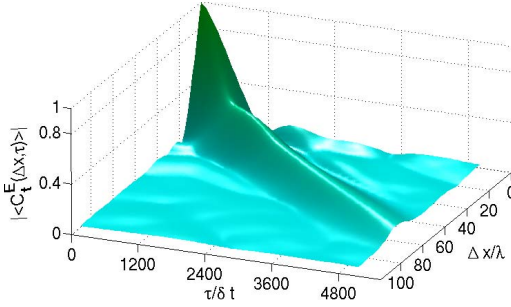


FIG. 5. (Color online) The average TDFC $|\langle C_t^E(\Delta x, \tau) \rangle|$ versus τ and Δx for random strength $u=0.15$.

$E(x, \omega)$ possesses similar structure in the spectrum between the different locations.

B. Spatial TDFC for $\tau \neq 0$

Now the issue comes to whether we can find a way to remove the cancellation between the different localized modes. After transforming $C_t^E(x_1, x_2, \tau)$ into the frequency domain, we get

$$\begin{aligned} C_t^E(x_1, x_2, \tau) &= \frac{\int E^*(x_1, \omega) E(x_2, \omega) e^{-i\omega\tau} d\omega}{\sqrt{\int |E(x_1, \omega)|^2 d\omega} \sqrt{\int |E(x_2, \omega)|^2 d\omega}} \\ &= \frac{1}{2} \frac{\sum_i f_i(x_1) f_i(x_2) (e^{ik_i(x_1-x_2)} + e^{-ik_i(x_1-x_2)}) e^{-i\omega_i\tau}}{\sqrt{\sum_i |f_i(x_1)|^2} \sqrt{\sum_i |f_i(x_2)|^2}}. \end{aligned} \quad (9)$$

We find that there is an offset phase $\omega_i\tau$ for each k_i . If there is a certain τ_p which makes $k_i(x_1-x_2) + \omega_i\tau_p = 0$ or $k_i(x_1-x_2) - \omega_i\tau_p = 0$ hold for arbitrary k_i , we get

$$\begin{aligned} C_t^E(x_1, x_2, \tau_p) &= \frac{\int E^*(x_1, \omega) E(x_2, \omega) e^{-i\omega\tau_p} d\omega}{\sqrt{\int |E(x_1, \omega)|^2 d\omega} \sqrt{\int |E(x_2, \omega)|^2 d\omega}} \\ &= \frac{1}{2} \frac{\sum_i f_i(x_1) f_i(x_2) (1 + e^{\pm i2k_i(x_1-x_2)})}{\sqrt{\sum_i |f_i(x_1)|^2} \sqrt{\sum_i |f_i(x_2)|^2}}. \end{aligned} \quad (10)$$

The second term on the right-hand side of Eq. (10) is mainly determined by the width of spontaneous spectrum, whereas the first term is related to the localization length ξ tightly.

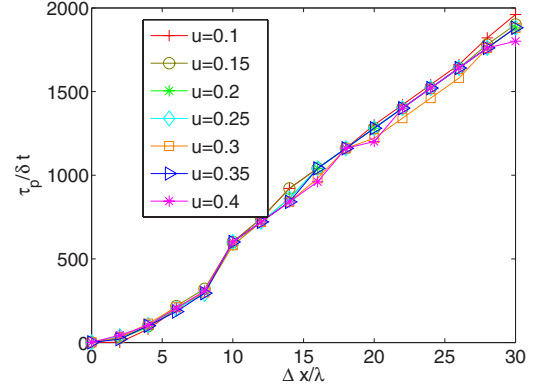


FIG. 6. (Color online) τ_p varied with Δx for different random strengths u .

Obviously, $|C_t^E(x_1, x_2, \tau)|$ will reach the maximum at $\tau = \tau_p$ because of the cancellation of the first term on the right-hand side of Eq. (10) diminishing. If $|\langle C_t^E(\Delta x, \tau) \rangle|$ versus τ and Δx is plotted, there will be a ridge.

In the following, we will validate the above discussion. Figure 5 shows $|\langle C_t^E(\Delta x, \tau) \rangle|$ versus τ and Δx for the random strength $u=0.15$. As we see from Fig. 5, there is a ridge indeed, whose projection into Δx and τ plane is shown in Fig. 6, in which the projections for other random strength u are also plotted. When Δx is larger than a certain value, Δx is linearly increased with τ_p , while the linear relation cannot be held when Δx approaches zero. This is because the second term on the right-hand side of Eq. (10) has considerable impact on $C_t^E(x_1, x_2, \tau_p)$ in the small- Δx region. In addition, we do not show τ_p varied with Δx for $u=0.45$ and $u=0.5$ because their ridges are not very prominent.

For the case that $|C_t^E(x_1, x_2, \tau)|$ approaches the maximum at $\tau_p = \pm k_i(x_1 - x_2) / \omega_i$, we can take another perspective: the fields at the different locations (x_1, x_2) at instant t include the component at instant $t - \tau_p$ of each other; thus, we can define a field-exchange speed (FES) $v_{ft} = \Delta x / \tau_p$. Table I shows v_{ft} for different u .

The mean value of the field-exchange speed v_{ft} is $0.625C$, and its root mean square is $0.0043C$. The ratio of them is 0.7% . Obviously, the field-exchange speed v_{ft} is almost not affected by the random strength u . In order to probe into the physical inheritance of the FES, various attempts are tried. In the end, we find that the FES is almost the group velocity of the period structure corresponding to the random system (namely, the structure of random strength $u=0$). By the transfer matrix method, we get the group velocity in the vicinity of the frequency ω_0 which is $0.632C$. The difference between the FES and the group velocity of the period structure is only 1.1% . We know that the localized mode is a dynamic equilibrium state. The question is how the state is preserved and how to characterize it. Here, we think it is just the field

TABLE I. The field-exchange speed v_{ft} for different random strengths u .

u	0.1	0.15	0.2	0.25	0.3	0.35	0.4
$v_{ft} (C)^a$	0.623	0.628	0.620	0.624	0.628	0.621	0.632

^aLight speed in vacuum.

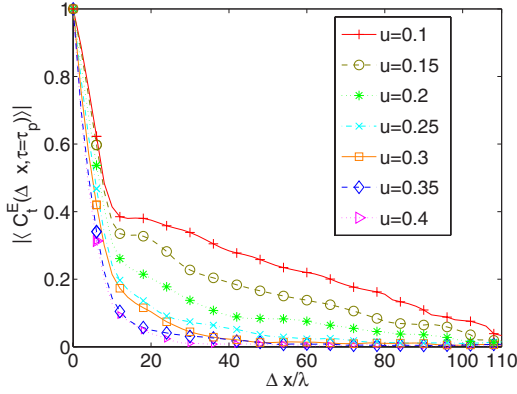


FIG. 7. (Color online) The average TDFC $|\langle C_t^E(\Delta x, \tau=\tau_p) \rangle|$ varied with spatial interval Δx for different random strengths u .

exchange (or, in other words, photon exchange) which preserves the localization of modes, and the dynamic property of localized modes can be characterized by the FES just as its static property is characterized by the localization length. It should be noted that this does not mean there exists energy transfer. This is very like a bottle of air; the molecules keep on moving though the whole is localized. Furthermore, we can infer that, with stronger difference of the refractive indices, the pumping threshold for the random system will decrease, because the FES will decrease with the difference of the refractive indices (just as the group velocity does) and the localized mode with slower FES will obtain more gain. This has already been shown theoretically and experimentally.^{28,29}

$|\langle C_t^E(x_1, x_2, \tau=\tau_p) \rangle|$ varied with Δx for different random strengths u and the correlation length of $C_t^E(x_1, x_2, \tau=\tau_p)$ versus the localization length ξ are shown in Figs. 7 and 8, respectively. Here, the correlation length is defined as $L_c = \int_0^\infty |\langle C_t^E(x_1, x_2, \tau=\tau_p) \rangle| d\Delta x$. As we see from Figs. 7 and 8, the increase of the correlation length with the localization length is sensitive and monotonous; this further confirms that the cancellation between the different localized modes can be removed by the offset phase $\omega_i \tau_p$.

IV. ENERGY-SPECTRUM CORRELATION

In the aspect of characterizing the localization length, the TDFC is very complex, thus we propose another correlation

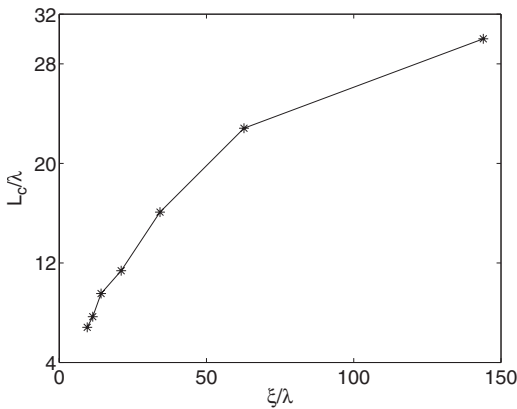


FIG. 8. The correlation length of $C_t^E(x_1, x_2, \tau=\tau_p)$ versus the localization length.

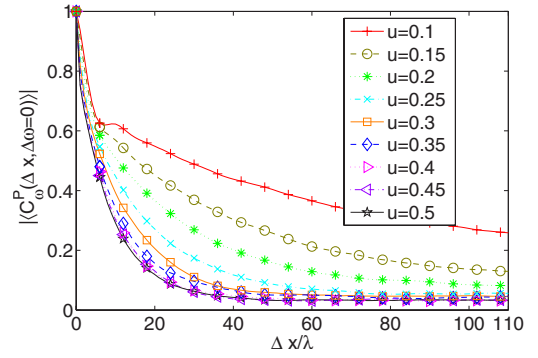


FIG. 9. (Color online) The average ESC $|\langle C_\omega^P(\Delta x, \Delta\omega=0) \rangle|$ varied with spatial interval Δx for different random strengths u .

(i.e., ESC) defined by Eq. (2). For $\Delta\omega=0$, it follows that

$$\begin{aligned} C_\omega^P(x_1, x_2, \Delta\omega=0) &= \frac{\int |E(x_1, \omega)|^2 |E(x_2, \omega)|^2 d\omega}{\sqrt{\int |E(x_1, \omega)|^4 d\omega \int |E(x_2, \omega)|^4 d\omega}} \\ &= \frac{\sum_i f_i^2(x_1) f_i^2(x_2) [2 + \cos(2k_i \Delta x)]}{3 \sqrt{\sum_i |f_i(x_1)|^4 \sum_i |f_i(x_2)|^4}}. \end{aligned} \quad (11)$$

In Eq. (11), the limitation of summation on the terms containing random phase φ_i to be zero has been used. From Eq. (11), we can know that $C_\omega^P(x_1, x_2, \Delta\omega=0)$ is directly relative to localization length ξ ; no need to offset phase $k_i \Delta x$ similar to Sec. III. The average ESC $\langle C_\omega^P \rangle$ depending on the different random strengths u is investigated according to Eq. (2) for $\Delta\omega=0$. The calculating procedure is the same as Sec. III; we generate a random configuration corresponding to a certain specified random strength u , add some sources of random spontaneous emission, and simulate it with the FDTD algorithm. In the end, we process the simulation results by Eq. (2) instead. For each random strength u , we average over 20 configurations at least. After the average, the correlations are also a function of Δx . Figure 9 shows that the average ESC $|\langle C_\omega^P(\Delta x, \Delta\omega=0) \rangle|$ varies with spatial interval Δx , and Fig. 10 shows the correlation length L_c of $C_\omega^P(x_1, x_2, \Delta\omega=0)$ versus the localization length ξ . Similar to Sec. III, the correlation length L_c of $C_\omega^P(x_1, x_2, \Delta\omega=0)$ is defined as $L_c = \int_0^\infty |\langle C_\omega^P(\Delta x, \Delta\omega=0) \rangle| d\Delta x$. Just as we see from Figs. 9 and 10, the average ESC becomes more and more strong as the random strength increases; its correlation length approximately linearly increases with the localization length. Here, the random phase inducing decorrelation in TDFC has diminished. Obviously, ESC is more convenient than TDFC in characterizing localization length, which means that we can determine the localization length by ESC in experiments. In addition, we also notice that ESC has inherent relation with TDFC. After some transformations and deductions, we can get

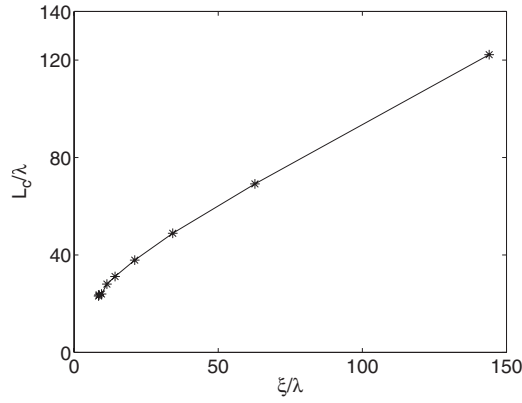


FIG. 10. The correlation length of $C_{\omega}^P(x_1, x_2, \Delta\omega=0)$ versus the localization length.

$$\begin{aligned}
 & C_{\omega}^P(x_1, x_2, \Delta\omega) \\
 &= \frac{\int_{-\infty}^{\infty} C_t^{E*}(x_1, x_1, \tau) C_t^E(x_2, x_2, \tau) d\tau}{\sqrt{\int_{-\infty}^{\infty} |C_t^E(x_2, x_2, \tau)|^2 d\tau \int_{-\infty}^{\infty} |C_t^E(x_1, x_1, \tau)|^2 d\tau}} \\
 &= \frac{\int_{-\infty}^{\infty} C_t^{E*}(x_1, x_1, \tau) C_t^E(x_2, x_2, \tau) d\tau}{\sqrt{\tau_{1c} \tau_{2c}}}, \quad (12)
 \end{aligned}$$

where τ_{1c}, τ_{2c} is coherence time at x_1, x_2 , respectively. So it follows that the ESC is the correlation of time-domain field autocorrelation.

V. CONCLUSION

In summary, under Anderson localization, the TDFC and ESC of spontaneous emission in one-dimensional random

media are investigated by numerical and theoretical methods in the present paper. For $\tau=0$, the correlation length of TDFC is unrelated with the random strength u . The reason has been discussed in detail in Sec. III. Briefly, it is the cancellation between the different localized modes that makes the dependence of the correlation length of the TDFC on the random strength disappear. After removing the cancellation between the different localized modes, the increase of the correlation length of $\max_{\tau} |C_t^E(\tau)|$ with the localization length is sensitive and monotonous. In particular, we demonstrate that the localized mode is a dynamic equilibrium state by investigation of the TDFC. Although the energy of the localized mode is localized, the fields at the different locations keep on exchanging with each other at a certain fixed speed. In fact, this is exactly the appearance of causality. The field-exchange speed is almost not affected by the random strength; its magnitude is very close to the group velocity of the corresponding periodic structure. The difference between them is about 1.1%. We think that the localization length does not sufficiently characterize the localized modes, while the field-exchange speed is a very useful parameter which can characterize the dynamic property of the localized mode. Furthermore, we can infer that, with a stronger difference of the refractive indices, the pumping threshold for the random system will decrease. In addition, by investigation of the ESC for $\Delta\omega=0$, we obtain that there is an approximately linear relation between the spatial correlation length of the energy spectrum and the localization length. Obviously, in lieu of characterizing the localization length, the ESC is more convenient than the TDFC.

ACKNOWLEDGMENTS

This work has been supported by the NNSFC (Grant No. 10374096), SFMSBRP (Grant No. 2001CCA02800), CNK-BRSF(Grant No. 2006CB921701), and the CAS-BaiRen program.

*Electronic address: xyjiang@mail.sim.ac.cn

¹Ping Sheng, *Introduction to Wave Scattering, Localization, and Mesoscopic Phenomena* (Academic Press, San Diego, 1995).

²Patrick Sebbah, *Waves and Imaging through Complex Media* (Kluwer Academic, Dordrecht, 2001).

³P. W. Anderson, *Phys. Rev.* **109**, 1492 (1958).

⁴P. W. Anderson, *Rev. Mod. Phys.* **50**, 191 (1978).

⁵A. F. Ioffe and A. R. Regel, *Prog. Semicond.* **4**, 237 (1960).

⁶N. F. Mott, *Metal-Insulator Transitions* (Taylor & Francis, London, 1974).

⁷S. John, *Phys. Rev. Lett.* **53**, 2169 (1984).

⁸P. W. Anderson, *Philos. Mag. B* **52**, 505 (1985).

⁹S. John, *Phys. Rev. Lett.* **58**, 2486 (1987).

¹⁰M. P. van Albada, A. Lagendijk, and M. B. van der Mark, in *Analogies in Optics and Micro Electronics*, edited by W. van Haeringen and D. Lenstra (Kluwer, Dordrecht, 1990), p. 85.

¹¹Z. Ye and A. Alvarez, *Phys. Rev. Lett.* **80**, 3503 (1998).

¹²Z. Ye and H. Hsu, *Appl. Phys. Lett.* **79**, 1724 (2001).

¹³C. H. Kuo, K. K. Wang, and Z. Ye, *Appl. Phys. Lett.* **83**, 4247 (2003).

¹⁴Lucia Florescu and Sajeev John, *Phys. Rev. Lett.* **93**, 013602 (2004).

¹⁵X. Jiang and C. M. Soukoulis, *Phys. Rev. Lett.* **85**, 70 (2000).

¹⁶V. S. Letokhov, *Zh. Eksp. Teor. Fiz.* **53**, 1442 (1967).

¹⁷N. M. Lawandy, R. M. Balachandra, A. S. L. Gomes, and E. Sauvain, *Nature (London)* **368**, 436 (1994).

¹⁸R. Pnini and B. Shapiro, *Phys. Rev. B* **39**, 6986 (1989).

¹⁹Richard Berkovits and Shechao Feng, *Phys. Rep.* **238**, 135 (1994).

²⁰M. C. W. van Rossum and Th. M. Nieuwenhuizen, *Rev. Mod. Phys.* **71**, 313 (1999).

²¹P. Sebbah, B. Hu, A. Z. Genack, R. Pnini, and B. Shapiro, *Phys. Rev. Lett.* **88**, 123901 (2002).

²²B. Shapiro, *Phys. Rev. Lett.* **57**, 2168 (1986).

²³B. Shapiro, *Phys. Rev. Lett.* **83**, 4733 (1999).

²⁴A. Yamilov, S. H. Chang, A. Burin, A. Taflove, and H. Cao, *Phys.*

- Rev. B **71**, 092201 (2005).
- ²⁵Bahaa E. A. Saleh and Malvin Carl Teich, *Fundamentals of Photonics* (Wiley, New York, 1991).
- ²⁶Peijun Yao, Wei Li, Songlin Feng, and Xunya Jiang, Opt. Express **14**, 12295 (2006).
- ²⁷P. Sebbah, B. Hu, J. Klosner, and A. Z. Genack (unpublished).
- ²⁸Y. Ling, H. Cao, A. L. Burin, M. A. Ratner, X. Liu, and R. P. H. Chang, Phys. Rev. A **64**, 063808 (2001).
- ²⁹S. John and G. Pang, Phys. Rev. A **54**, 3642 (1996).